East European Journal of Physics. 4. 72-79 (2022)
DOI:10.26565/2312-4334-2022-4-05 ISSN 2312-4334

EXOTIC STRUCTURE OF ^{17}Ne-^{17}N AND ^{23}Al-^{23}Ne MIRROR NUCLEI†

Ruqaya A. Mohammed[a,*], Wasan Z. Majeed[a]
[a]*Department of Physics, College of Science, Baghdad University, Iraq*
**Corresponding Author E-mail: ruqayaahmed9@gmail.com*
Received September 10, 2022; revised September 11, 2022; accepted September 15, 2022

In terms of the core nucleus plus valence nucleon, shell-model calculations using two model spaces and interactions, the relationship between a nucleus' proton skin, and the difference in proton radii of mirror pairs of nuclei with the same mass number are investigated. In this work, two pairs of mirror nuclei will be studied: ^{17}Ne-^{17}N and ^{23}Al-^{23}Ne. For ^{17}Ne-^{17}N nuclei, p-shell and mixing of psd orbits are adopted with Cohen-Kurath (ckii) and psdsu3 interactions. While for ^{23}Al-^{23}Ne, the sd-shell and sdpf shell are adopted with the universal shell model (USD) and sdpfwa interactions. Also, the ground state density distributions, elastic form factors, and root mean square radii of these pairs' nuclei are studied and compared with available experimental data. . In general, it was found that the rms radius of the valence proton(s) is larger than that of the valence neutron(s) in its mirror nucleus. The results show that these nuclei have the exotic structure of a halo or skin.
Keywords: Mirror Nuclei, Proton and Neutron Skin Thickness, Density Distribution, Exotic Nucleus
PACS: 14.20.Dh21.10.Ft, 21.10.Gv, 21.10.Hw, 21.60.-n, 21.60.Cs

1. Introduction

The infinite lifetimes of stable nuclei and their relatively balanced Z to N ratios—which range from around 1 to roughly 1.5 – define them. There are around 300 of these nuclear types. Exotic or unstable nuclei are other nuclei whose total number is unknown. Through beta processes, the exotic nuclei decay to other nuclei where Z and N are more evenly balanced. Until a stable nucleus is created, this decay normally occurs successively. As a result, only stable nuclei exist on Earth, as opposed to exotic nuclei, which are figuratively exotic [1]. In nuclear physics, it is important to investigate the mirror nuclei that have an interchanged number of protons and neutrons because it directly addresses the isospin symmetry idea, which was described by Heisenberg in 1932 [2]. In the isospin explanation of the nuclear forces, the binding energies of the mirror nuclei should be similar, apart from Coulomb interaction. While if Coulomb's interaction is taken into account, the energy difference between two mirror nuclei has come from the electromagnetic interaction [3].

In order to characterize the charge radii, theoretical mean-field techniques such as the Hartree-Fock-Bogolyubov (HFB) method, the nuclear shell model, and different shell model approximations have been developed. Therefore, several updates to experimental charge radii databases in which around 1000 experimental data points have been analyzed and assembled [4, 5].

Nuclear structure studies have proven to benefit greatly from using electron-nucleus scattering. It has given us a great deal of knowledge, particularly regarding the charge density distributions of stable nuclei. Because of this, it is predicted that the new facilities at GSI [6, 7] and RIKEN [8–10] will offer a good opportunity to study the charge density, and consequently the proton density distribution, of exotic nuclei using elastic electron scattering. A physically effective indicator of the isovector characteristics of nuclear interactions is the neutron-skin thickness, which is a ground state parameter of the nucleus [11].

In addition, a rather interesting feature of studying the mirror nuclei is that the neutron skin thickness can be found through the knowledge of proton radii alone from the mirror pairs. It has recently been proposed that the difference between the charge radii of mirror nuclei is proportional to the neutron skin [12]. Various theoretical and experimental studies are conducted to investigate the properties of mirror nuclei [13, 14]. B.N. Giv and S. Mohammadi [15] (2017) calculated Coulomb displacement energies in mirror nuclei 49Mn and 49Cr and compared them with experimental data by using the shell model code. OXBASH A. Boso et al. [16] (2017) investigated mirror nuclei ^{23}Mg–^{23}Na by using the Mirror Energy Differences (MED) in up to high spin it is a direct result of the breaking of isospin symmetry. K. Arai et al. [17] (2018), investigated the structure of the mirror nuclei 9Be and 9B by using a completely antisymmetrized 9-nucleon wave function in a microscopic α+α+n and α+α+p three-cluster model.

There are two aims of this study. First, calculate the skin thickness through the knowledge of proton radii alone from the mirror pairs. Second, investigate the exotic structure of two pairs of mirror nuclei, ^{17}Ne-^{17}N and ^{23}Al-^{23}Ne, by studying the ground state properties like rms radii, density distribution, and form factors.

2. THEORY

The electron scattering form factors for the scattering of an electron from a target nucleus are given by [18]:

$$F_{J,t_z}(q)=\sqrt{\frac{4\pi}{2J_i+1}}\frac{1}{N_{t_z}}\left\langle J_f\left\|\sum_{i=1}^{N_{t_z}}\hat{T}_{J,t_z}(q,i)\right\|J_i\right\rangle F_{fs}(q)F_{cm}(q) \quad (1)$$

† ***Cite as:*** R.A. Mohammed, and W.Z. Majeed, East Eur. J. Phys. East Eur. J. Phys. **4**, 72 (2022), https://doi.org/10.26565/2312-4334-2022-4-05

J_i and J_f represent the nucleus' initial and final states, respectively, while N_{t_z} denoting the normalization factor. $F_{fs}(q)$ is the finite nucleon size correction and $F_{cm}(q)$ is the center of mass correction. The form of these corrections is [19,20]:

$$F_{fs}(q) = \left[1 + \left(q / 4.33\, fm^{-1} \right)^2 \right]^{-2}$$
$$F_{cm}(q) = e^{q^2 b^2 / 4A} \tag{2}$$

where q is the momentum transfer, A is the nuclear mass number and b is the harmonic-oscillator size parameter

The longitudinal multipole operator $\hat{T}_{J,t_z}$ is given by [18]:

$$\hat{T}_{J,t_z}(q,i) = \int d^3 r\, j_J(qr) Y_{JM}(\Omega) \hat{\rho}_{t_z}(\vec{r},i) \tag{3}$$

where the spherical Bessel's function is represented by $j_J(qr)$ and $\hat{\rho}_{t_z}(\vec{r},i)$ is the operator for the density of protons and neutrons, and is given by

$$\hat{\rho}_{t_z}(\vec{r},i) = \sum_{i=1}^{A} \delta(\vec{r} - \vec{r}_i) \tag{4}$$

Then, equation (4) is reduced to:

$$\hat{T}_{J,t_z}(q,i) = \sum_{i=1}^{A} j_J(qr_i) Y_{JM}(\Omega_i) \tag{5}$$

The reduced matrix element in equation (1) can be written as a sum over elements of the one body density matrix (OBDM) elements and the corresponding reduced single particle matrix element [21]

$$\left\langle J_f \left\| \sum_{i=1}^{N_t} \hat{T}_{J,tz} \right\| J_i \right\rangle = \sum_{ab} OBDM(J_f, J_i, a, b, J, t_z) \left\langle a \left\| \hat{T}_{J,t_z} \right\| b \right\rangle \tag{6}$$

where a and b label the single-particle states. The OBDM is defined as [21]

$$OBDM\left(J_f, J_i, a, b, J, t_z\right) = \frac{\left\langle J_f \left\| \left[a^{+}_{a,t_z} \otimes \tilde{a}_{b,t_z} \right]^{(J)} \right\| J_i \right\rangle}{\sqrt{2J+1}} \tag{7}$$

The reduced single-particle matrix elements of the Coulomb operator in equation (6) are given by

$$\left\langle a \left\| \hat{T}_J \right\| b \right\rangle = \int_0^{\infty} dr r^2 j_J(qr) \left\langle j_a \left\| Y_J \right\| j_b \right\rangle R_{n_a l_a}(r) R_{n_b l_b}(r) \tag{8}$$

Where $R_{nl}(r)$, is the radial single-particle wave functions. The Coulomb form factors given in equation (1) become:

$$F_{J,t_z}(q) = \frac{1}{N_{t_z}} \sqrt{\frac{4\pi}{2J_i+1}} \sum_{a,b} OBDM\ (J_i, J_f, a, b, J, t_z) \left\langle j_a \left\| Y_J \right\| j_b \right\rangle \int_0^{\infty} dr r^2 R_{n_a l_a}(r) R_{n_b l_b}(r) j_J(qr) F_{fs}(q) F_{cm}(q), \tag{9}$$

and can be written as

$$F_{J,t_z}(q) = \frac{4\pi}{N_{t_z}} \int_0^{\infty} dr r^2 \rho_g(r) j_J(qr) F_{fs}(q) F_{cm}(q), \tag{10}$$

where $\left\langle j_a \left\| Y_J \right\| j_b \right\rangle$ represents the reduced matrix element of the spherical Harmonics and $\rho_g(r)$ is nucleon density distribution and is given by [21]:

$$\rho_g(r) = \frac{1}{\sqrt{4\pi}} \sqrt{\frac{1}{2J_i+1}} \sum_{a,b} OBDM\left(J_i, J_f, a, b, J, t_Z\right) \left\langle j_a \left\| Y_J \right\| j_b \right\rangle R_{n_a l_a}(r) R_{n_b l_b}(r). \tag{11}$$

For the ground state $J=0$ density distribution, one has $J_i = J_f$ and $n_a = n_b$, $\ell_a = \ell_b$, $j_a = j_b$ The ground state density distribution takes the form:

$$\rho_g(r) = \frac{1}{\sqrt{4\pi}}\sqrt{\frac{1}{2J_i}+1}\sum_a OBDM(J_i, a, J=0, t_Z)\sqrt{2J_a+1}\left|R_{n_a l_a}(r)\right|^2 . \tag{12}$$

Finally, the corresponding elastic scattering $J=0$ form factor ($C0$) is written in the following form

$$F_{0.g}(q) = \frac{4\pi}{g}\int_0^\infty drr^2\rho_g(r)j_0(qr)\;\; F_{fs}(q)F_{cm}(q) . \tag{13}$$

The matter density distribution is given by [22]:

$$\rho_m(r) = \rho_{p+n}^{core}(r) + \rho_{p(n)}^{valence}(r) . \tag{14}$$

Therefore, the corresponding terms radii are given by

$$\langle r^2\rangle_N = \frac{4\pi}{N}\int_0^\infty drr^4\rho_N(r) \tag{15}$$

where N represents the corresponding number of nucleons in each case.

The neutron skin thickness $\Delta\left\langle r^2\right\rangle_n^{1/2}$ and the proton skin thickness $\Delta\left\langle r^2\right\rangle_p^{1/2}$ which are related to the difference between the neutron $\left\langle r^2\right\rangle_n^{1/2}$ and proton $\left\langle r^2\right\rangle_p^{1/2}$ rms radii for nuclei and their mirror as [11,16]:

$$\Delta\left\langle r^2\right\rangle_n^{1/2} = \left\langle r^2\right\rangle_n^{1/2} - \left\langle r^2\right\rangle_p^{1/2} , \tag{16}$$

$$\Delta\left\langle r^2\right\rangle_p^{1/2} = \left\langle r^2\right\rangle_p^{1/2} - \left\langle r^2\right\rangle_n^{1/2} . \tag{17}$$

Considering the effects of charge-dependent and Coulomb contributions are turned off, for mirror nuclei, the neutron radius of a nucleus (Z, N) is the same as the proton radius of its mirror nucleus (Z,N) [11], then:

$$\Delta\left\langle r^2\right\rangle_{mirror}^{1/2} = \left\langle r^2\right\rangle_p^{1/2}(N,Z) - \left\langle r^2\right\rangle_p^{1/2}(Z,N) . \tag{18}$$

Eq. (17) represents the important method to determine neutron and proton skins using charge radii of mirror pairs nuclei.

3. RESULTS AND DISCUSSION

Proton, neutron, core, valence and matter radii, density distributions, and electron scattering form factors of two pairs mirror nuclei ^{17}Ne-^{17}N and ^{23}Al-^{23}Ne are calculated in the framework of a shell model using core plus valence calculations with different model space and two harmonic-oscillator size parameters. One of these parameters is for core nucleons (b) to reproduce the core radius and the other for the outer nucleon(s) (b_v) to reproduce the rms matter radius. The nuclear Shell model calculations were performed with shell model code OXBASH [23], where the one body density matrix (OBDM) elements of the core parts are obtained.

For ^{17}Ne-^{17}N ($J^\pi T$= 1/2$^-$ 3/2) nuclei, the theoretical calculation using the shell model takes two ways. Firstly, the Cohen–Kurath interaction CKII [24] is used. The configurations $(1s_{1/2})^4$ $(1p)^{11}$ are used for the core nucleons ^{15}O ($J^\pi T$= 1/2$^-$ 1/2) and ^{15}N ($J^\pi T$= 1/2$^-$ 1/2). The values of the oscillator size parameter (b) equal to 1.61 fm for ^{15}O and b = 1.6 fm for ^{15}N are chosen to reproduce the experimental rms radii. The outer two nucleons in this pair of mirror nuclei are assumed to be in a pure $1d_{5/2}$. To reproduce the matter radii of ^{17}Ne-^{17}N different values of the oscillator size parameter (b_v) are chosen for the extra nucleons b_v = 2.45 fm for ^{17}Ne and b_v =1.61 fm for ^{17}N. These values of b_v give the matter radii agree with the measured values as shown in Table 1.

Secondly, the mixing of the *psd* orbits is used with the psdsu3 interaction [25]. All core nucleons in ^{15}O and ^{15}N are considered to be active in all orbits in *psd* shells. The harmonic-oscillator size parameter, b = 1.75 fm is used for core nucleons ^{15}O and 1.57 fm for ^{15}N. While the outer nucleons which are assumed to be in $1d_{5/2}$ orbit have the values b_v = 2.43 fm for ^{17}Ne and b_v = 1.59 fm for ^{17}N. These values give the proton, neutron, valence, core, and matter radii in agreement with the measured value [26] as shown in Table 1, where the experimental and calculated rms radii for these nuclei are displayed.

Regarding ^{23}Al-^{23}Ne ($J^\pi T$ = 5/2$^+$ 3/2) pair nuclei, the theoretical calculations are the same way as in ^{17}Ne-^{17}N nuclei but with different model space and interactions. Firstly, the configurations $(1s_{1/2})^4$ $(1p)^{12}$ plus 7 nucleons moved in *sd* orbits are used for the core nucleons ^{22}Mg ($J^\pi T$ = 0$^+$ 1) and ^{22}Ne ($J^\pi T$ = 0 $^+$1). In *sd* model space all orbits in 2s-1d shells are considered where the universal shell model USD [27] is used. To reproduce the core radii a value of b = 1.74 fm is used for ^{22}Mg and ^{22}Ne. While the outer nucleon must be in $1d_{5/2}$ with value b_v = 3.4 fm for ^{23}Al and b_v =1.75 fm for ^{23}Ne.

Secondly, the sdpfwa [28] interaction is used for the core of ^{23}Al - ^{23}Ne nuclei with configuration $(1s_{1/2})^4$ $(1p)^{12}$ plus 7 nucleons moved in *sdpf* orbits are used for the core nucleons ^{22}Mg ($J^{\pi}T= 0^{+}$ 1) and ^{22}Ne ($J^{\pi}T= 0$ $^{+}$1). A value of b = 1.7 fm is used for ^{22}Mg and ^{22}Ne. while the values b_v = 3.45 fm and b_v = 1.72 fm are used for the outer nucleon (which is assumed to be in a pure $1d_{5/2}$) in ^{23}Al and ^{23}Ne, respectively. All values of b and b_v give the rms proton, neutron, valence, core, and matter radii in agreement with the measured value as shown in Table 1, where the experimental and calculated rms radii of two pairs of mirror nuclei are displayed. It is evident from this Table that for both interactions, the calculated rms radii and the experimental data coincide quite well.

Table 1. The values of rms proton $\langle r^2\rangle_p^{1/2}$, neutron $\langle r^2\rangle_n^{1/2}$, core $\langle r^2\rangle_c^{1/2}$, valence $\langle r^2\rangle_v^{1/2}$ and matter $\langle r^2\rangle_m^{1/2}$ radii in fm for ^{17}Ne-^{17}N and ^{23}Al-^{23}Ne mirror nuclei

Nucleus		rms (fm)				
		$\langle r^2\rangle_p^{1/2}$	$\langle r^2\rangle_n^{1/2}$	$\langle r^2\rangle_c^{1/2}$	$\langle r^2\rangle_v^{1/2}$	$\langle r^2\rangle_m^{1/2}$
^{17}Ne	Ckii	2.97	2.39	2.4	4.58	2.75
	psdsu3	2.98	2.38	2.41	4.54	2.75
	Exp.[26]	2.97(7)	2.69(7)	2.44(4)	-	2.75(7)
^{17}N	Ckii	2.39	2.54	2.4	2.99	2.48
	psdsu3	2.38	2.55	2.41	2.97	2.48
	Exp.[26]	-	-	2.42(1)	-	2.48(5)
^{23}Al	Usd	3.25	2.75	2.8	6.36	3.04
	Sdpfwa	3.21	2.68	2.73	6.45	2.99
	Exp.[26]	3.1(25)	2.634(23)	2.78(26)	-	2.91(25)
^{23}Ne	Usd	2.75	2.87	2.8	3.27	2.822
	Sdpfwa	2.68	2.81	2.73	3.21	2.76
	Exp.[26]	-	-	2.95(36)	-	2.76(4)

The values of valence nucleon radii $\langle r^2\rangle_v^{1/2}$ is very essential to studying the differences between the pairs of mirror nuclei. The calculations indicate that the different model space and interactions gives nearly linear dependence between $\langle r^2\rangle_v^{1/2}$ and the mass number. As shown in Fig. 1 with the increase in mass number, the values of the valence-proton(s) and valence-neutron(s) nuclei seem to be in two separate lines. For ^{17}Ne and ^{23}Al nuclei, the $\langle r^2\rangle_v^{1/2}$ values are larger than those for ^{17}N and ^{23}Ne nuclei, since the halo phenomenon in ^{17}Ne and ^{23}Al nuclei is connected to the outer proton(s) which give large rms radii.

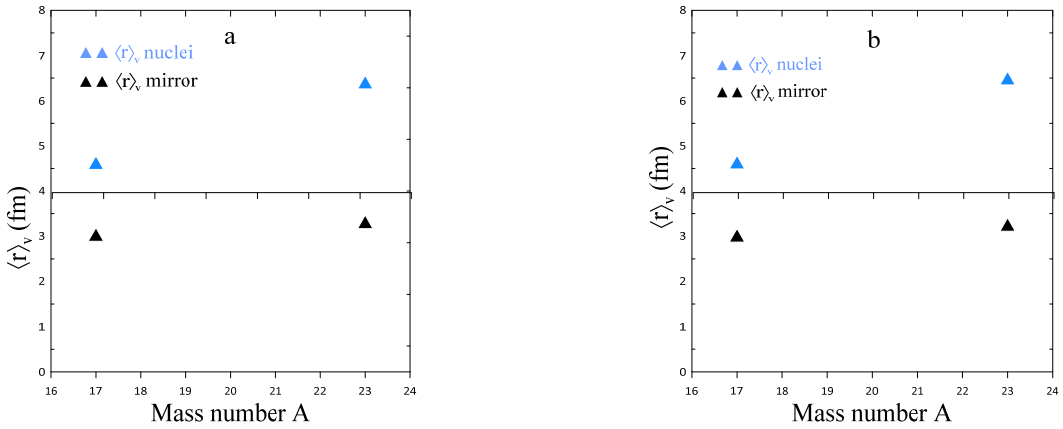

Figure 1. The last nucleon(s) rms radius is calculated with (a) ckii (usd) interaction and (b) psdsu3 (sdpfwa) interaction as a function of mass number

Along with the increase in mass number A, there is also a linear increase in the difference between the valence proton and valence neutron values. With experimental data for both model spaces, one may plot $\langle r^2\rangle_m^{1/2}$ as a function of the mass number, as seen in Fig. 2, in order to compare the size of the exotic structure between mirror nuclei more clearly. This figure showed that both interactions give good agreement with experimental data. Also, it can be seen that the $\langle r^2\rangle_m^{1/2}$ values of ^{17}Ne and ^{23}Al nuclei are consistently larger than those of their respective mirror partners (^{17}N and ^{23}Ne) and almost in two different lines because the halo structure and the outer proton(s) halo in ^{17}Ne and ^{23}Al nuclei is weakly bound. In addition, with an increase in the mass number A of the nucleus, the exotic size difference between every pair of mirror nuclei increases.

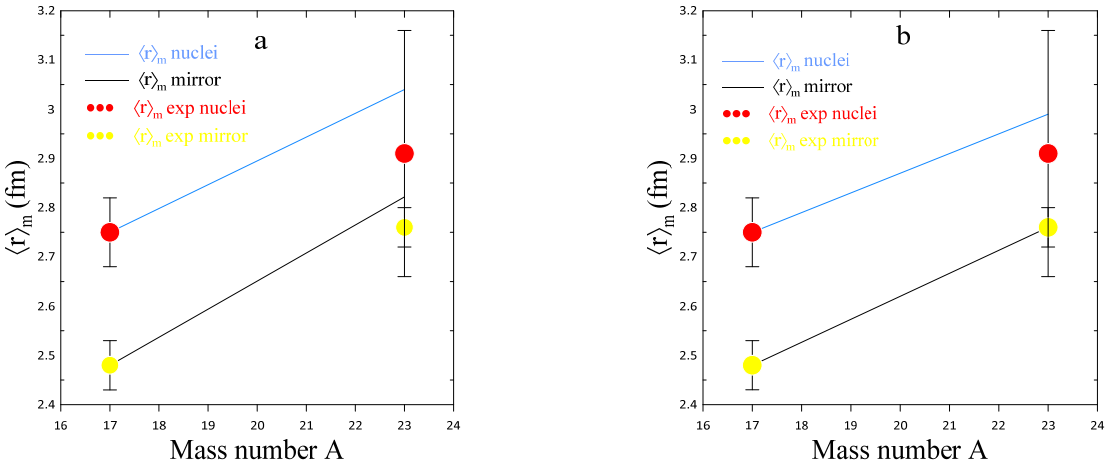

Figure 2. The calculated matter radii with (a) ckii (usd) interaction and (b) psdsu3 (sdpfwa) interaction as a function of mass number compared with the experimental data [29,30]

The results for the proton skins $\Delta\langle r^2\rangle_p^{1/2}$, neutron skins $\Delta\langle r^2\rangle_n^{1/2}$ of the corresponding mirror nuclei and $\Delta\langle r^2\rangle_{mirror}^{1/2}$ in fm are given for the both model space and interactions in Table 2. It is noticed that the proton-skin thickness for a certain proton excess (Z-N) is greater than the neutron-skin thickness for the same degree of neutron excess (N-Z). The protons' Coulomb repulsion is clearly to blame for this. As noted in Table 2, there is little difference between the predicted proton skin values and the interactions and model space considered during these studies. In particular, the values of $\Delta\langle r^2\rangle_p^{1/2}$ obtained with psdsu3 (sdpfwa) interactions are larger than those with ckii (usd) interactions.

Table 2. Predicted proton skins $\Delta\langle r^2\rangle_p^{1/2}$, neutron skins $\Delta\langle r^2\rangle_n^{1/2}$ of the corresponding mirror nuclei and $\Delta\langle r^2\rangle_{mirror}^{1/2}$ in fm

Nucleus	$\Delta\langle r^2\rangle_p^{1/2}$		Mirror	$\Delta\langle r^2\rangle_n^{1/2}$		$\Delta\langle r^2\rangle_{mirror}^{1/2}$	
	Ckii	psdsu3		Ckii	psdsu3	Ckii	psdsu3
^{17}Ne	0.58	0.6	^{17}N	0.15	0.17	-0.58	-0.6
^{23}Al	USD	sdpfwa	^{23}Ne	USD	sdpfwa	USD	sdpfwa
	0.5	0.53		0.12	0.13	-0.5	-0.53

In order to investigate the differences between ground state properties of the mirror nuclei, the proton and neutron density distributions of two pairs of mirror nuclei are displayed in Figs. 3 and 4. Two model spaces and interactions are considered in these calculations, ckii (usd) interaction calculations are shown in part (a) in these figures and part (b) for psdsu3 (sdpfwa) interactions. The red solid and dashed curves in these figures are the calculated proton density and the blue solid and dashed curves represented the neutron density. These figures demonstrate how the calculated proton density of halo nuclei differs from the calculated neutron density of their mirror nuclei because the outer proton density is higher than that of the outer neutron in its mirror nucleus. These graphs make it clear that there are significant long tails in the density distribution of the (^{17}Ne, ^{23}Al) nuclei, which correspond to the halo structure of these nuclei.

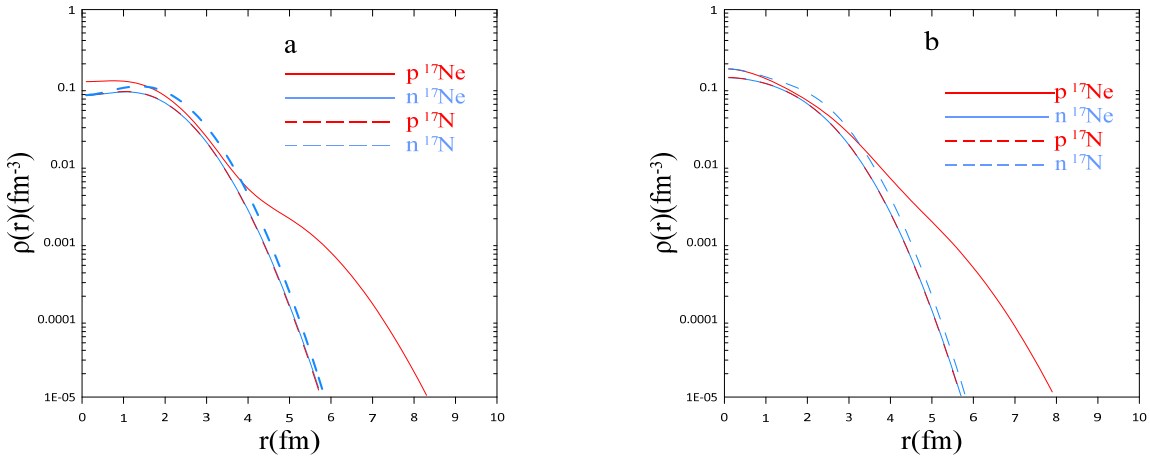

Figure 3. Proton and neutron density distributions of ^{17}Ne – ^{17}N mirror nuclei (a) for ckii (b) for psdsu3.

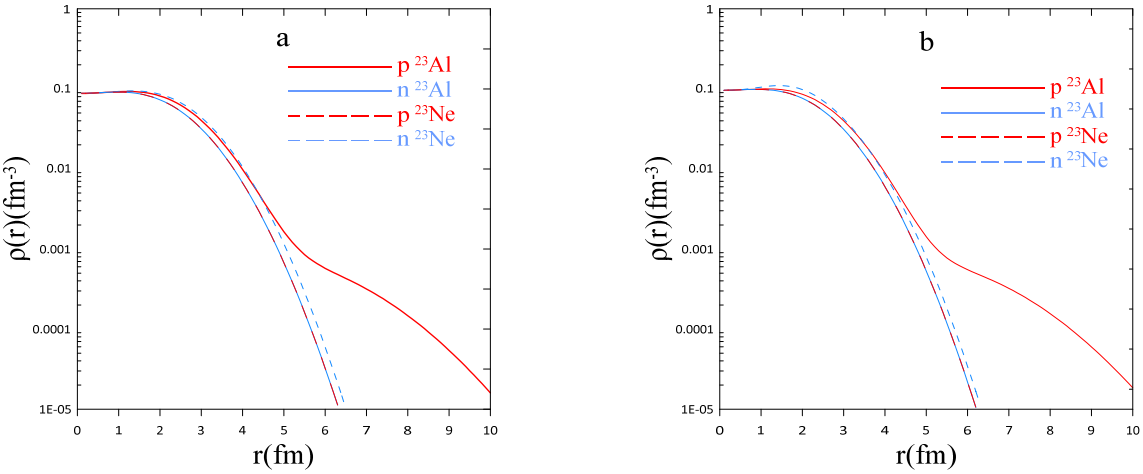

Figure 4. Proton and neutron density distributions of ^{23}Al - ^{23}Ne mirror nuclei (a) for usd , (b) for sdpfwa

The matter density distributions $\rho_m(r)$ of ^{17}Ne-^{17}N and ^{23}Al-^{23}Ne nuclei are displayed in Figures (6a) and (6b) respectively. The solid curve (blue and black) in this figure is the calculated matter density of the nuclei and their mirror obtained with the *p (sd)* model space. The dashed curve is the calculated matter density with *psd* (*psdf*) model space. The filled circles are the experimental nucleon density. It is evident from these figures that the calculated matter density distribution for both model space are in good accordance with that of the fitted data, at $r \leq 5$ fm for ^{17}Ne-^{17}N.

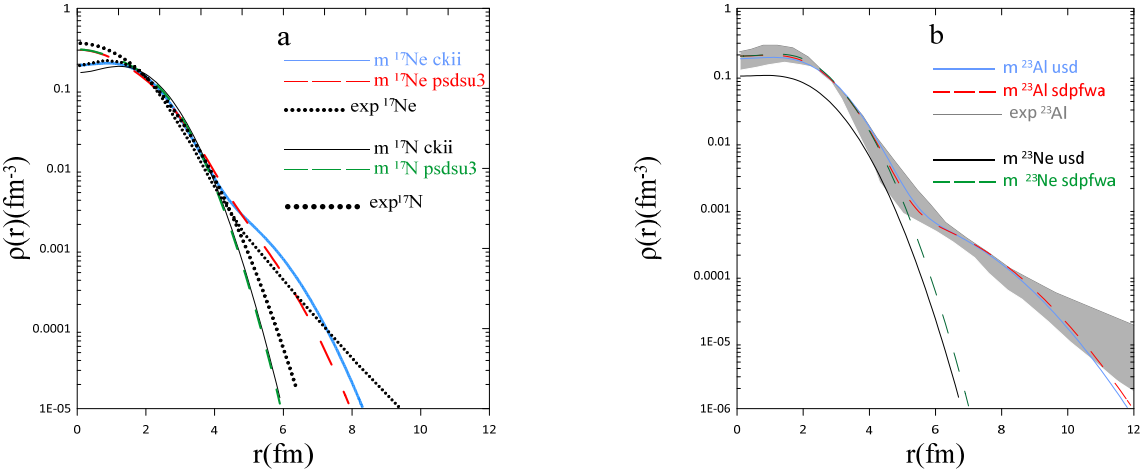

Figure 5. Matter density distributions (a) for ^{17}Ne-^{17}N, (b) for ^{23}Al-^{23}Ne mirror nuclei [31, 32]

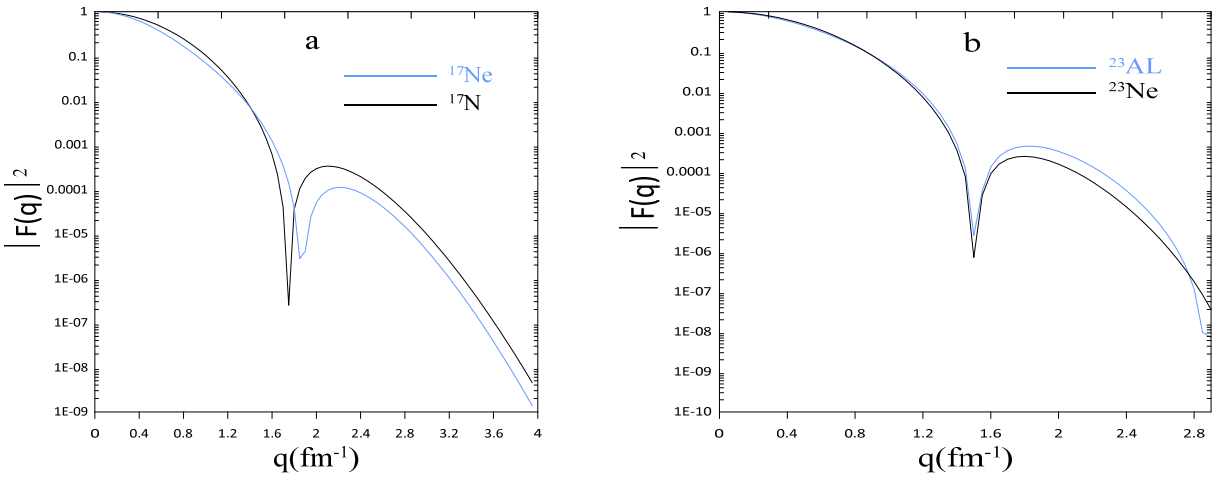

Figure 6. Elastic form factors (a) for ^{17}Ne-^{17}N, (b) for ^{23}Al-^{23}Ne mirror nuclei

Finally, For the sake of completeness of the comparison, elastic form factors of two pairs of nuclei are calculated using Plane Wave Born Approximation (PWBA). To compare the results of the form factor of the halo nuclei with that of their mirror nuclei, we present the calculated *C*0 form factor using ckii interaction for ^{17}Ne-^{17}N and usd interaction

for ^{23}Al-^{23}Ne nuclei as shown in Figure 6. It is seen from this figure that the charge form factors of the pairs of mirror nuclei are different. Comparing the result of these nuclei, show that the form factors are sensitive to the change of the tail part of the proton density since the ground state proton density is connected with the *C*0 form factor. As one can see that each black curve and the blue curve in the figures have one diffraction minimum and one diffraction maximum. Also, because the center of mass correction varies depending on the mass number and the size parameter b, there is a discrepancy between the form factors of mirror nuclei.

4. CONCLUSIONS

The relationship between a nucleus' proton skin and the difference between the proton radii of the mirror pair is seen in the current work. Each pair of mirror nuclei has different sizes in terms of their nuclear size, and these differences get linearly larger with increasing mass number A for both interactions. The rms radius of the valence proton was also discovered to be greater than that of the valence neutron in its mirror nucleus. In addition, the results of density distributions show that the two pairs of mirror nuclei have exotic structures. Finally, the form factor is sensitive to the change of the proton density, since the ground state proton density is connected with the C0 form factor and the difference between the form factors of these nuclei is due to the mass correction which depends on the size parameter b.

ORCID IDs

Ruqaya A. Mohammed, https://orcid.org/0000-0002-6501-453X; **Wasan Z. Majeed,** https://orcid.org/0000-0001-6595-1841

REFERENCE

[1] T. Otsuka, "Emerging concepts in nuclear structure based on the shell model," Physics, **4**(1), 258 (2022). https://doi.org/10.3390/physics4010018

[2] H. Jian, Y. Gao, F. Dai, J. Liu, X. Xu, C. Yuan, K. Kaneko, ,*et al*, "β-Delayed γ Emissions of 26P and Its Mirror Asymmetry," Symmetry, **13**(12), 2278, (2021). https://doi.org/10.3390/sym13122278

[3] G. Agnelli, Master Degree in Physics, Universita Degli Studi di Milano, 2019. https://www0.mi.infn.it/~jroca/doc/thesis/thesis-giancarlo-agnelli.pdf

[4] I. Angeli, and K. P. Marinova, "Table of experimental nuclear ground state charge radii: An update," At. Data Nucl. Data Tables, **99**(1), 69 (2013). https://doi.org/10.1016/j.adt.2011.12.006

[5] M. Bao, Y. Lu, Y. M. Zhao, and A. Arima, "Predictions of nuclear charge radii," Phys. Rev. C, **94**(6), (2016). https://doi.org/110.1103/PhysRevC.94.064315

[6] H. Simon, "The ELISe experiment at FAIR," Nucl. Phys. A, **787**(1–4), 102 (2007). https://doi.org/10.1016/j.nuclphysa.2006.12.020

[7] A.N. Antonov et al., "The electron–ion scattering experiment ELISe at the International Facility for Antiproton and Ion Research (FAIR) – A conceptual design study," Nucl. Instruments Methods Phys. Res. Sect. A Accel. Spectrometers, Detect. Assoc. Equip., **637**(1), 60 (2011). https://doi.org/10.1016/j.nima.2010.12.246

[8] T. Suda, and M. Wakasugi, Prog. Part. Nucl. Phys. **55**, 417 (2005). https://doi.org/10.1016/j.ppnp.2005.01.008

[9] T. Motobayashi, and H. Sakurai, "Research with fast radioactive isotope beams at RIKEN," Prog. Theor. Exp. Phys. **2012**(1), 2012. https://doi.org/10.1093/ptep/pts059

[10] M. Wakasugi *et al.*, "Construction of the SCRIT electron scattering facility at the RIKEN RI Beam Factory," Nucl. Instruments Methods Phys. Res. Sect. B Beam Interact. with Mater. Atoms, **317**, 668 (2013).

[11] M.K. Gaidarov, I. Moumene, A.N. Antonov, D.N. Kadrev, P. Sarriguren, and E.M. de Guerra, "Proton and neutron skins and symmetry energy of mirror nuclei," Nucl. Phys. A, vol. 1004, p. 122061, 2020. https://doi.org/10.1016/j.nuclphysa.2020.122061

[12] A. Boso, S.M. Lenzi, F. Recchia, J. Bonnard, S. Aydin, M.A. Bentley, B. Cederwall, *et al*, "Isospin symmetry breaking in mirror nuclei 23mg-23Na," Acta Phys. Pol. B, **48**(3), 313 (2017). https://doi.org/10.5506/APhysPolB.48.313

[13] J. Ekman, D. Rudolph, C. Fahlander, R.J. Charity, W. Reviol, D.G. Sarantites, V. Tomov, *et al*, "The A = 51 mirror nuclei 51Fe and 51Mn," Eur. Phys. J. A, **9**(1), 13 (2000). https://doi.org/10.1007/s100500070050

[14] K. Wimmer, W. Korten, P. Doornenbal, T. Arici, P. Aguilera, A. Algora, T. Ando, *et al.*, "Shape Changes in the Mirror Nuclei Kr 70 and Se 70," Phys. Rev. Lett. **126**(7), 2021. https://doi.org/10.1103/PhysRevLett.126.072501

[15] B.N. Giv, and S. Mohammadi, "Calculating Energy Levels in ^{49}Mn/^{49}Cr Mirror Nuclei with OXBASH Code," Comput. Biol. Bioinforma, **5**(5), 70 (2017), https://doi.org/10.11648/j.cbb.20170505.13

[16] F. Sammarruca, "Proton skins, neutron skins, and proton radii of mirror nuclei," Front. Phys. Front. Phys. 6, 90 (2018). https://doi.org/10.3389/fphy.2018.00090

[17] K. Arai, Y. Ogawa, Y. Suzuki, and K. Varga, "Structure of the mirror nuclei 9Be and 9B in a microscopic cluster model," Phys. Rev. C - Nucl. Phys. 54(1), 132 (1996). https://doi.org/10.1103/PhysRevC.54.132

[18] T. De Forest, Jr., and J. D. Walecka, "Electron scattering and nuclear structure", Adv. Phys. **15**, 1 (1966). https://doi.org/10.1080/00018736600101254

[19] J.P. Glickman, W. Bertozzi, T.N. Buti, S. Dixit, F.W. Hersman, C.E. Hyde-Wright, M.V. Hynes, *et al.*, "Electron scattering from Be 9", Phys. Rev. C, **43**(4), 1740 (1991). https://doi.org/10.1103/PhysRevC.43.1740

[20] R.A. Radhi, "Perturbative role in the inelastic electron scattering from 29Si", Eur. Phys. J. A, **A34**, 107 (2007). https://doi.org/10.1140/epja/i2007-10488-0

[21] B.A. Brown, R. Radhi, and B. H. Wildenthal, Physics Reports, **101**(5), 313 (1983). https://doi.org/10.1016/0370-1573(83)90001-7

[22] R.A. Radhi, A.K. Hamoudi, and W.Z. Majeed, "Calculation of The Nuclear Matter Density Distributions and Form Factors For The Ground State of P", Iraqi J. Sci. **54**(2), 349 (2013). https://www.iasj.net/iasj/download/47f853b71cc4457e

[23] B.A. Brown et al., Oxbash for Windows PC (MSU-NSCL report number 1289) 1 (2005).

[24] S. Cohen, and D. Kurath, Nucl. Phys. **73**, 1 (1965). https://doi.org/10.1016/0029-5582(65)90148-3
[25] J.P. Elliott, Proc. Roy. Soc. A, **245**, 1240 (1958). https://doi.org/10.1098/rspa.1958.0072
[26] A. Ozawa, T. Suzuki, and I. Tanihata, "Nuclear size and related topics," Nucl. Phys. A, **693**(1–2), 32 (2001). https://doi.org/10.1016/S0375-9474(01)01152-6
[27] B.A. Brown, and B.H. Wildenthal, Ann. Rev. Nucl. Part. Soi. **38**, 29 (1988). https://doi.org/10.1146/annurev.ns.38.120188.000333
[28] E.K. Warburton, J.A. Becker, and B.A. Brown, "Mass systematics for A=29–44 nuclei: The deformed A∼32 region", Phys. Rev. C, **41**, 1147 (1990). https://doi.org/10.1103/PhysRevC.41.1147
[29] R.N. Panda, M. Panigrahi, M.K. Sharma, and S.K. Patra, "Evidence of a Proton Halo in 23Al: A Mean Field Analysis," Phys. At. Nucl. **81**(4), 417 (2018). https://doi.org/10.1134/S1063778818040154
[30] K. Riisager, "Halos and related structures," Phys. Scr. **2013**, 014001 (2013). https://doi.org/10.1088/0031-8949/2013/T152/014001
[31] K. Tanaka, M. Fukuda, M. Mihara, M. Takechi, D. Nishimura, T. Chinda, T. Sumikama, *et al*, "Density distribution of ^{17}Ne and possible shell-structure change in the proton-rich sd-shell nuclei," Phys. Rev. C, **82**(4), 44309 (2010). https://doi.org/10.1103/PhysRevC.82.044309
[32] F. De-Qing, M. Chun-Wang, M. Yu-Gang, C. Xiang-Zhou, C. Jin-Gen, C. Jin-Hui, G. Wei, *et al*, "One-Proton Halo Structure in ^{23}Al," Chinese Phys. Lett. **22**(3), 572 (2005). https://doi.org/10.1088/0256-307X/22/3/015

ЕКЗОТИЧНА СТРУКТУРА ДЗЕРКАЛЬНИХ ЯДЕР ^{17}Ne–^{17}N ТА ^{23}Al–^{23}Ne

Рукая А. Мохаммед[a], Васан З. Маджид[a]
[a]Фізичний факультет, Науковий коледж, Багдадський університет, Ірак

З точки зору ядра плюс валентного нуклона, досліджуються розрахунки моделі оболонки з використанням двох модельних просторів і взаємодій, взаємозв'язок між протонною оболонкою ядра та різницею радіусів протонів дзеркальних пар ядер з однаковим масовим числом. У даній роботі будуть досліджені дві пари дзеркальних ядер: ^{17}Ne - ^{17}N і ^{23}Al - ^{23}Ne. Для ядер ^{17}Ne - ^{17}N прийнято p-оболонку та змішування psd-орбіт із взаємодіями Коена-Курата (ckii) та psdsu3. У той час як для ^{23}Al - ^{23}Ne оболонки sd і sdpf прийнято з універсальною моделлю оболонки (USD) і взаємодіями sdpfwa. Також досліджуються розподіли густини основного стану, пружні формфактори та середньоквадратичні радіуси ядер цих пар та порівнюються з наявними експериментальними даними. Загалом було виявлено, що середньоквадратичний радіус валентного протона(ів) більший, ніж радіус валентного нейтрона(ів) у його дзеркальному ядрі. Результати показують, що ці ядра мають екзотичну структуру гало або шкіри.

Ключові слова: дзеркальні ядра, товщина оболонки протонів і нейтронів, розподіл густини, екзотичне ядро